Fiber-Metal Laminate Panels Reinforced with Metal Pins

Ruham Pablo Reis, Iaroslav Skhabovskyi,
Alberto Lima Santos, Leonardo Sanches,
Edson Cocchieri Botelho and Américo Scotti

Additional information is available at the end of the chapter

Abstract

Fiber-metal laminates (FMLs) are key to modern composite structures and metal-composite coupling is crucial to improve their effectiveness. Cold-metal transfer (CMT) PIN welding, in correlated efforts, has been successfully explored as a metal-composite hybrid joining approach. This work proposes a novel development on FMLs, which consists of introducing metal pins welded by CMT PIN for anchoring their metal and composite layers together. Thus, miniaturized FML panels with different pin deposition spacing and patterns are evaluated with emphasis in drop-weight testing followed by buckling and by means of Iosipescu shear test as complement. They are also subjected to cosmetic and preliminary modal analyses. Besides not adding significant weight, the pins does not make the panels more brittle and their distribution does not imply significant effect in the capacity that the panels have to dissipate impact. The panels with pins exhibit a less catastrophic trend, indicating damage tolerance improvement as significantly higher loads at longer axial displacements in buckling test after impact are achieved. The anchoring effect of the pins is confirmed throughout the shear test results. The pins also significantly increase the damping factor of the panels and the changes in their metal surfaces by the CMT PIN process are considered as irrelevant.

Keywords: fiber-metal laminates, composite structures, adhesion, anchoring, CMT PIN

1. Introduction

The demand for high-performance-lightweight structures continues to stimulated advances in fiber- metal laminates (FMLs). Cortes and Cantwell [1] describe FMLs as hybrid composite structures based on thin sheets of metal alloys and plies of fiber-reinforced polymeric

materials. Sinmazçelik et al. [2] justify this combination by considering that metals are isotropic materials, have high strength and impact resistance and are easy to repair, while full composites generally present high strength and stiffness and excellent fatigue characteristics. According to Salve et al. [3], FMLs take positive characteristics from both metals and fiber-reinforced composites, resulting in superior mechanical properties compared to conventional lamina processed from fiber-reinforced composites or monolithic metals. Despite exhibiting low weights, according to Seydel and Chang [4], composite materials are very susceptive to impact damage. On the other hand, metals are in general heavier, but might have excellent impact resistance. Thus, very light and impact resistant panels might be produced by combining the low volumetric mass density of a fiber-reinforced polymer with the high impact resistance of ductile metals. As stated by Vlot [5], impact damage zones of FMLs are smaller than those found in fiber-reinforced composites alone. In summary, FMLs are characterized by a balance of low structural weight and high strength and stiffness, when compared with metals.

The adhesion between metal and composite is clearly a crucial factor to improve the effectiveness of FMLs and several techniques accomplish it by changing the surface characteristics of the metal part [2]. In this line, hybrid joining approaches have been developed, but specifically aiming at improving the performance of composite-metal joints [6]. These approaches essentially rely on macro-scale metal anchorages on the metal surface to interlock the layers of fiber-reinforced polymer and add strength to the adhesive bond. One of the most recent techniques applies an array of pins deposited on the metal part, before joining, as anchorages (mechanical interlocking) for the composite part. Cold-metal transfer (CMT) PIN, an arc-welding-based process developed and commercialized by Fronius (Austria), would be a relatively low-cost option to be used. The CMT PIN was created from its parent process called CMT, in which metal wire is continuously fed and an electric arc (protected by gas) is open between the wire tip and the material to be welded, as in all gas metal arc welding (GMAW) techniques. But in difference to common GMAW, CMT uses a proprietary torch, which periodically reverses the advancing electrode wire when it touches the weld pool, allowing a smooth transfer of molten material into it (in this instant, current is also considerably reduced, with no short-circuit current peaks) without spattering (loss of material). The heat transferred to the work piece is very low, causing just minor metallurgical changes as well as low levels of distortion and discoloration/oxidation (including in the reverse side) in the base metal. The CMT PIN embarks a program for pin depositions. Following short-circuiting, it causes the wire to stay resting against the weld pool (with no arc) allowing time for cooling and consequent welding of the wire to the base metal. Shortly afterwards, a low current is forced to heat and soften the welded wire near its mid length (between the torch and the work piece), but not enough to break it apart and open the arc. With the reversing motion started, the soft wire undergoes a tensile force and is broken, leaving a pin formed on the base metal. By changing deposition parameters, pins of different sizes and geometries can be formed [7]. Ucsnik et al. [8] have shown that pins deposited by CMT PIN on the metal side improved the strength of metal-composite joints. According to Graham et al. [9], adhesive bonding with CMT PIN anchorage was able to consistently outperform adhesive bonded only specimens in terms of strength and energy absorption at quasi-static and high loading rates, as well as in terms of damage tolerance after impact, environmental durability and mechanical fatigue performance.

The capacity that the CMT PIN process seems to have to enhance the performance of composite-metal hybrid joints might be extended to FMLs. Arrays of pins on the metal sides could perform as anchorages for the composite sides throughout the panels, contributing to the

performance along with the adhesive bonding between the composite and metal sheets. This approach has been recently investigated for the first time and the initial results are promising [10], despite the first pinned panels, due to manufacturing issues related to the number of prepreg layers, have exhibited significant variation in thickness. The first results indicate that the pins have potential to improve damage tolerance of fiber-metal laminate panels (FMLPs). Thus, the objective of this present work was to assess the application of metal pins deposited by CMT PIN on metal surfaces used as layers of FMLPs, yet controlling the thickness and the number of prepreg layers. The methodological approach includes comparing small-sized FMLPs with different pin deposition patterns and spans to a reference (without pins) FMLP, in terms of energy dissipation during drop-weight testing, impact damage characterization and buckling test after impact. Iosipescu shear test, modal analysis and cosmetic characterization were also carried out.

2. Methodological approach

2.1. Manufacturing of the panels

The small-sized FMLPs reinforced with metal pins were produced as illustrated in **Figure 1**. The reference FMLPs (without pins) were produced in the same way, with exception of the pin deposition step. The metals parts were composed of AISI 430 stainless steel sheets (350 × 80 × 0.4 mm). For pin deposition, a Fronius TransPuls Synergic 5000 power source was used, connected to a VR7000-CMT wire feeder, a PullMig CMT torch and a RCU 5000i remote control unit, with DB0875 data base selected (synergic line CrNi 19 9 PIN). A welding robot was used to move the torch according to the deposition pattern. An AWS ER309L filler wire with nominal diameter of 1 mm (verified value of 0.98 ± 0.00 mm) was used as pin material and Ar with 4% (verified as 3.7%) of CO_2 gas at a flow rate of 8 L/min was employed to protect the pin deposition. Fronius Contec MD® contact tips were employed, as recommended for CMT PIN. The torch was always kept perpendicular to the metal parts. The metal surfaces were all homogeneously wiped with acetone wetted cloth. Other input parameters, such as contact-tip to work-piece distance (5 mm), metal sheet temperature (room temperature ≈ 27°C) and pin deposition sequence were remained unchanged. The CMT PIN process was then parameterized to get minimum-height (considering the thickness of the FMLs) and small ball-head pins. Ucsnik et al. [8] had shown that the ball-head shaped pins present potential in metal-composite hybrid joining. Pins of 2.50 ± 0.06 mm in height and 1.40 ± 0.03 mm in head diameter were produced, resulting in an average pin weight of 0.023 ± 0.002 g.

The pin deposition process was monitored by sampling the electrical current and voltage data, as exemplified in **Figure 2**. The pin deposition cycle (T) was 5.73 s, consequence of the robot motion between two consecutive deposition points, which was not optimized in this work. As seen, the CMT PIN process works basically by controlling the levels of current applied to the electrode-wire and the dwell time in each level. First, the voltage is at its open-circuit level ready for arc starting. Then, the electrical arc is struck (by short-circuiting the electrode-wire to the base metal) and its tip and base metal below are melted (t_{arc} = 0.04 s). Subsequently, after the electrode-wire forward movement and contact with the base metal, the arc is extinguished and the welding between the electrode-wire and the base metal takes place (t_{weld} = 0.02 s).

Finally, the welded electrode-wire undergoes heating, softening and breaking apart at its mid length range by a combination of current flow and electrode-wire backward movement (t_{rup} = 0.36 s).
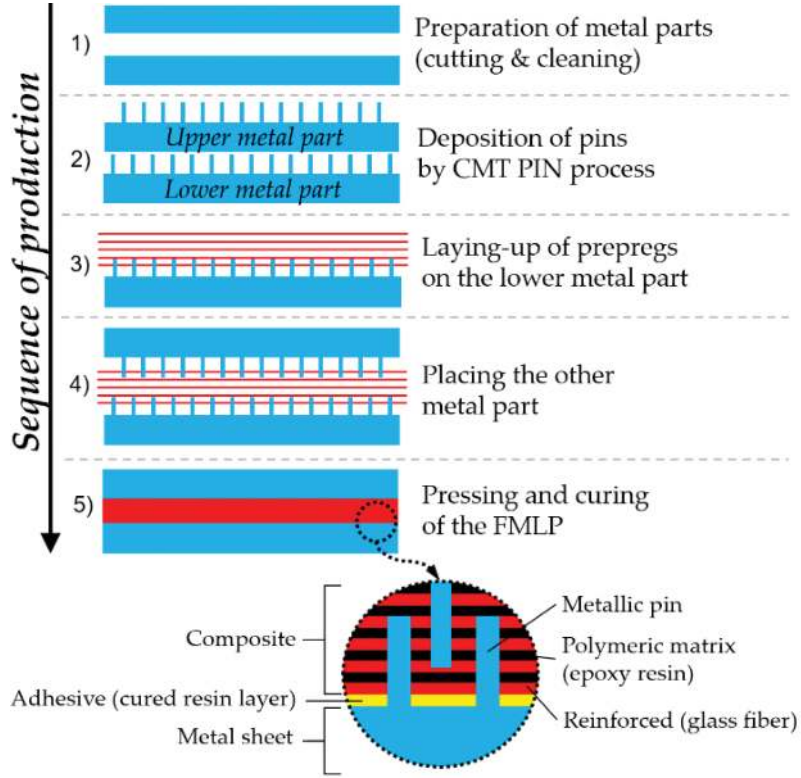

Figure 1. Sequence of production of small-sized FMLPs reinforced with metal pins welded by cold-metal transfer (CMT) PIN process.
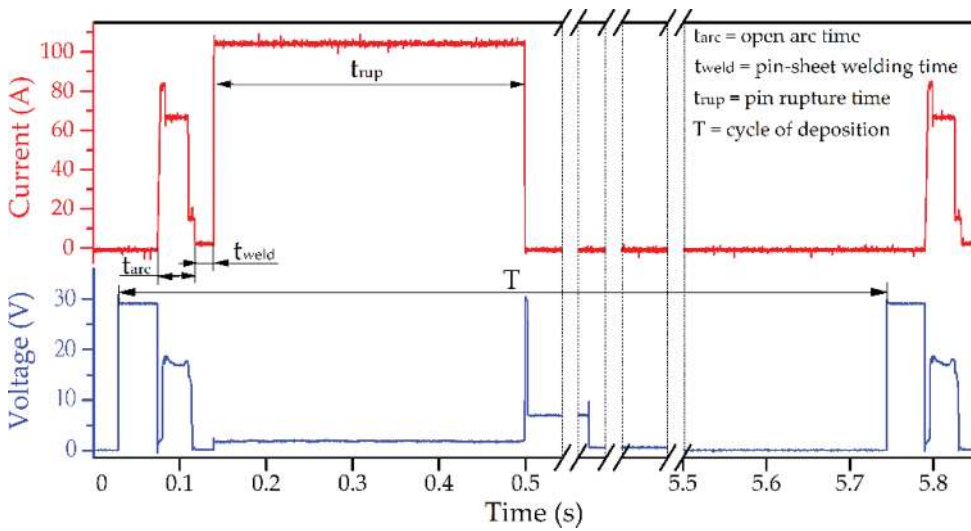

Figure 2. Cycle of pin deposition based on the electrical current and voltage data.

After CMT PIN processing, all metal parts (with and without pins) went through ultrasonic cleaning by immersion in acetone for 8 minutes to remove any process-related or not elements that could impair the adherence of the composite parts (**Figure 3**). For composite lamination, prepregs made of glass fiber (8-Harness Satin Weave) and epoxy resin from Hexcel Corporation (product data 7781-38"-F155) were employed. Each layer of prepreg was cut with dimensions of 360 × 90 mm (in excess of 5 mm measured from each of the metal sheet edges). The prepreg layers were stacked on top of the lower metal parts (with or without pins), always aligning the warp yarns with their length and, consequently, the filling yarns with their width. Next, the upper metal parts were placed aligned to the prepreg layers and lower metal parts. All prepreg handling was executed in a white room, avoiding to the maximum any contamination. All small-sized panels were wrapped with a thin film of release agent (polyamide) and then processed in groups of three in a CARVER® CMG100H-15-C hot-curing press according to the curing cycle displayed in **Figure 4**. After curing, the composite material exciding the edges of each panel was removed by means of band sawing followed by belt sanding, ending up in panels of 350 × 80 × 4 mm.

Figure 3. Example of metal sheet after pin deposition, where: (a) before; and (b) after cleaning.
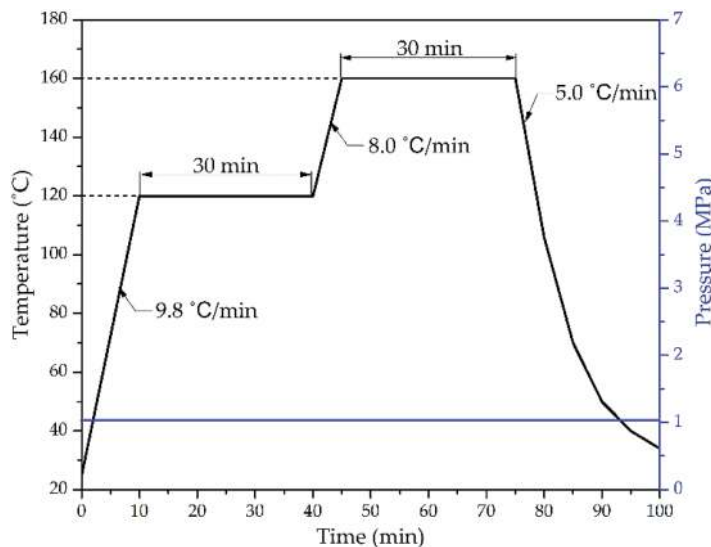

Figure 4. Curing cycle used for the fabrication of the small-sized FMLPs.

Two basic types of small-sized FMLPs were made (**Figure 5**): conventional FMLPs (without pins), i.e., metal-composite-metal (M-C-M); and FMLPs with pins, i.e., pined metal-composite-pined metal (MPin-C-MPin). The MPin-C-MPin type was produced using a combination of two levels of pin separation (5 and 10 mm) and two deposition patterns (hexagonal and squared). The pins of the upper metal parts were deposited with an adequate displacement in relation to the pins of the lower metal parts, avoiding contact between the upper and lower pins and providing homogenous distribution. Each one of the five small-sized FMLPs types was produced twice for replication in the tests.
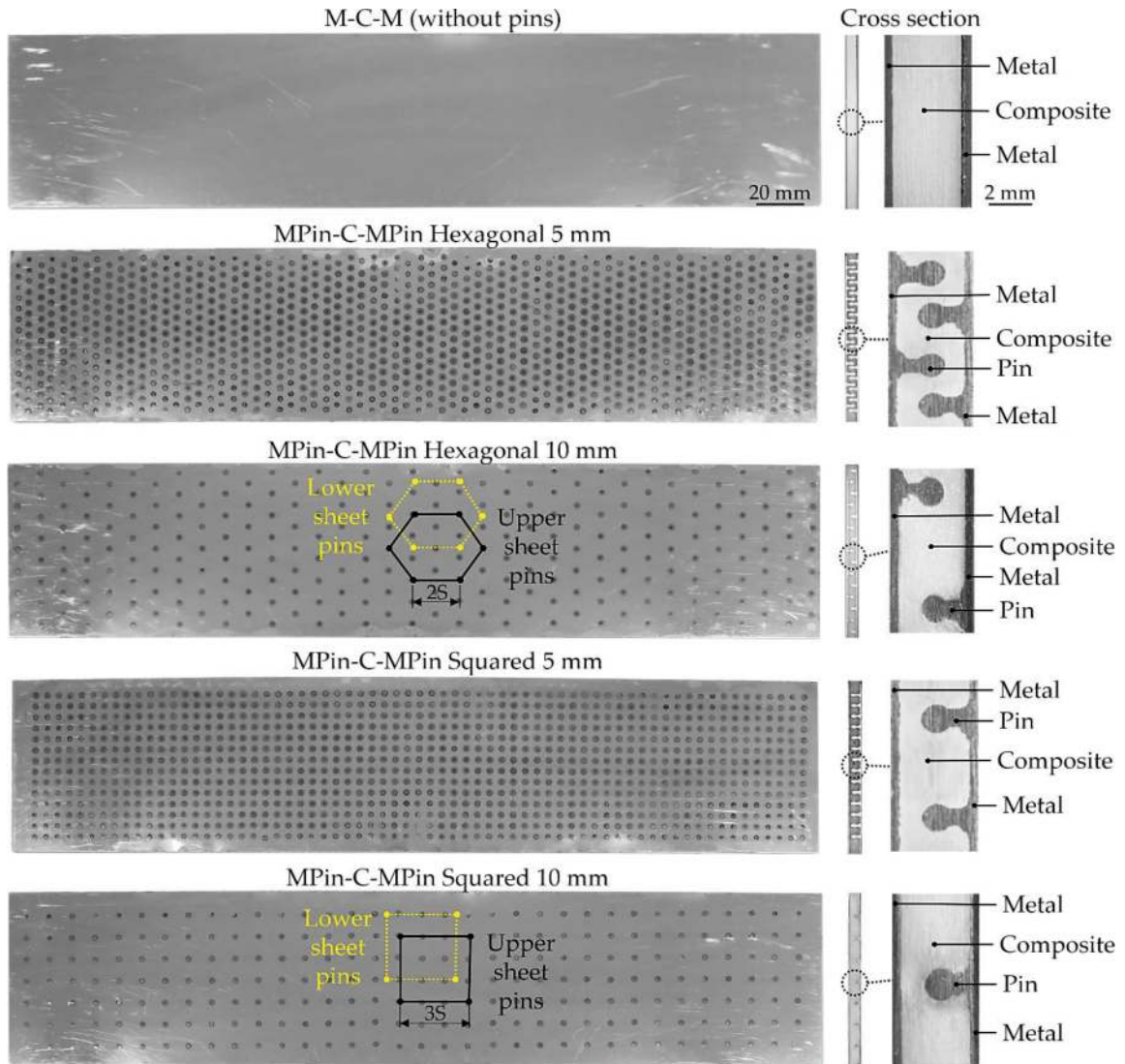
Figure 5. Types of small-sized panels fabricated with respective cross sections and schematic overlapping of pins on the upper and lower metal sheets, where M-C-M stands for metal-composite-metal, MPin-C-MPin for pined metal-composite-pined metal for hexagonal and squared pattern and S for distance separating the pins (panel width ≈ 80 mm; panel length ≈ 350 mm; the dot-like marks on the panels with pins are due to stainless steel heat-induced oxidation right under where the pins were deposited—This esthetic effect could be avoided with inert gas back purging).

Panel type	Pins per panel	Prepreg layers per panel	Actual thickness (mm)	Pin density (pin/cm²)	Mass density (g/cm³)
M-C-M (without pins)	0	13	3.90 ± 0.03	0	3.0
MPin-C-MPin hexagonal 5 mm	2001	13	4.04 ± 0.03	3.61	3.3
MPin-C-MPin hexagonal 10 mm	525	13	4.00 ± 0.07	0.94	3.0
MPin-C-MPin squared 5 mm	1976	13	4.08 ± 0.01	3.57	3.3
MPin-C-MPin squared 10 mm	518	13	3.96 ± 0.02	0.93	3.1

Table 1. Characteristics of the small-sized FMLPs.

As shown in **Table 1**, an attempt was made to keep the same thickness (approximately 4 mm) and prepreg layers per panel (13) for all FMLPs types. Pin density was estimated for each pertinent case, by considering the respective number of pins divided by the panel surface area (560 cm²). However, concerning mass density, usually crucial for FMLPs, the presence of pins has only marginal effect, regardless of pin density. The overall average mass density of the FMLPs with pins was 3.2 g/cm³, close to the case of M-C-M (without pins).

3. Non-destructive evaluation

3.1. Modal analysis

Modal analysis is a tool largely used to determine dynamic properties (natural frequencies, damping factors and vibration modes) of mechanical structures by imposing vibrations [11]. According to Rao [12], any movement of a flexible structure that repeats itself after a time interval is called vibration. This movement can be inferred instantaneously or continuously. The use of modal analysis is often applied due to the ease of implementation, relatively low cost, as well as being a nondestructive analysis.

According to Bolina et al. [13], the natural frequencies (fn) indicate the rate of free oscillation of the structure, after ceasing the force that caused its movement. In other words, it represents how much the structure vibrates when there is no longer a force applied to it. It is worth recalling that the value of the natural frequency of a structure depends on its stiffness and mass. In a structure several natural frequencies can be observed because it can vibrate freely (after being excited by a force) in several directions and modes. In practice, higher values of natural frequency indicate that elastic stresses are preponderant to inertial forces. Moreover, whenever a structure oscillates with a frequency equal to one its natural frequencies, a phenomenon called resonance occurs. The resonance implies high amplitudes of vibration, and can cause structural failures as, for example, in the breaking of a crystal glass of wine due to sound energy. In this case, when the frequency of vibration caused by the source

(sound wave) coincides with the natural frequency of the crystal glass, the amplitude of oscillation of this body reaches high values, because the source progressively gives energy to the body, and the crystal glass might break if the strain extensions exceed the levels supported by the material. However, vibration levels during a resonance can be attenuated if there are dissipation mechanisms that have high damping factors present in the structure, for example, shock absorbers (holding tightly the crystal glass in one's hand avoid the resonance-induced breakage). A more damped structure at a certain natural frequency can attenuate vibration levels more quickly. The damping factors (ξn) represent the damping levels of a structure, which in turn are characterized for each of its natural frequencies.

By analyzing, for a given natural frequency (periodic movement) the relationship between the points that discretize the structure, one obtains the natural modes of vibration. That is, the modes of vibration determine the way the structure vibrates at a certain natural frequency. In practice, by knowing the dynamic properties of a structure, it is possible to determine how the vibration oscillations will be at different measurement positions. Therefore, the objective of applying experimental modal analysis in the FMLPs was to evaluate, through the respective natural frequencies (fn) and damping factors (ξn), whether the pins inside the FMLPs would be able to modify the dynamic properties of the panels. The modal forms of the FMLPs were not evaluated in this work.

According to Lundkvist [14], structural dynamic properties or modal parameters in practice are identified from the Frequency Response Function (FRF). To obtain the FRF, the data that are in time domain are transformed to frequency domain, using the Fourier transformation, as exemplified in **Figure 6**. At the same time, from the response of the system vibrating under a condition, the modal properties are determined. It can be said that from the identified modal properties, the dynamic temporal behavior of the structure is predicted under any excitation conditions. As shown in **Figure 6(d)**, a temporal response of the structure contains the participation of its modes of vibration, each mode of vibration contemplating a natural frequency, damping factor and modal form. In order to apply the modal analysis in the small-sized panels, the experimental bench shown in **Figure 7** was used.

Some details of the experimental bench assembly are given below:

- The small-sized FMLP is hung by means of a nylon line glued to the side edges of it, forming a 60 mm arrow, as shown in **Figure 8**. It is called a "free-free" boundary condition when there is no rigid support or fixation of the structure. In this way, FMLP would be, by this experimental setup, in a "free-free" boundary condition, which was chosen because it is relatively simple to perform and quite informative.

- The positions of analysis of the dynamic response of each panel were based on a mesh of 51 points, as also indicated in **Figure 8**.

- The piezoelectric accelerometer is a model 352C22 (S/N LW181487) from the manufacturer PCB Piezotronics®, fixed in a position of the small-sized FMLP by means of a specific wax, that allows the propagation of the vibrations between the panel and the acceleration.

- The shaker is a model K2007E01 from manufacturer Modal Shop Inc. with the function of programming time and frequency of vibration to induce in the object of analysis (panel) through a connection tube. In this work, the shaker was programmed to produce a white noise type signal (random signal with equal intensity at different frequencies) comprising the frequency range 0–800 Hz in order to find the dynamic properties of the structure. The choice of this frequency range was made from a preliminary study, in which the first four modes of vibration were found. This frequency band determines the composition of the white noise that will be exerted by the electromagnetic exciter.

- The load cell is a model 208C03 (S/N LW34448), glued to the panel at a given position, as shown in **Figure 8**.

- The data acquisition system is capable of obtaining and analyzing the accelerometer and load cell signals. This system was configured to obtain a frequency resolution (Δf) of 0.25 Hz and an analysis band between 0 (fmin) and 800 (fmax) Hz. The acquisition rate (temporal resolution) of the data is then defined automatically by the acquisition system.

- The software is from Brüel and Kjær, from the manufacturer Vibrant Technology®, for acquisition and post-processing to identify the dynamic properties parameters of the panels.
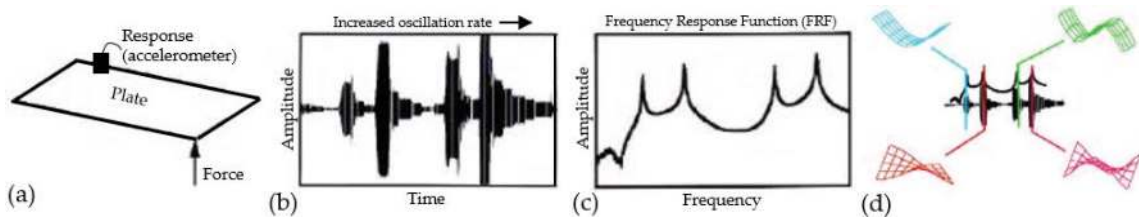

Figure 6. Illustration of a modal analysis, where: (a) experimental assembly; (b) response of the plate in the time domain; (c) response of the plate in the frequency domain (FRF); (d) overlap of the responses and example of the modal plate forms corresponding to each natural frequency (resonance) (after [15]).
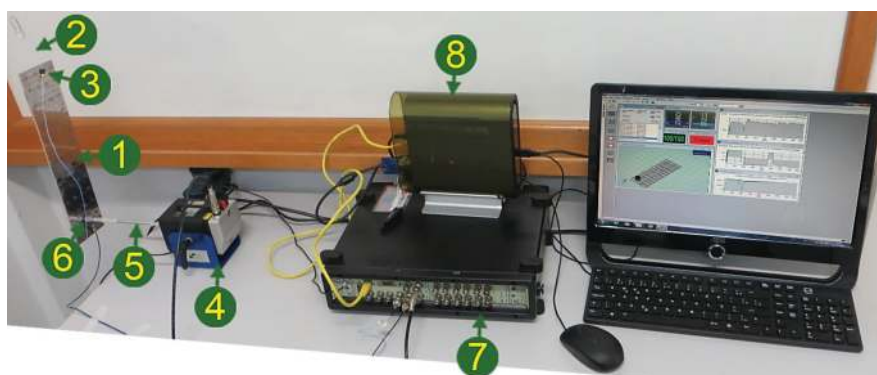

Figure 7. Experimental bench with the equipment used for perform modal analysis of the small-sized FMLPs, where: 1—panel (object of analysis); 2—nylon line glued to the edges of the FMLP; 3—accelerometer; 4—shaker; 5—stinger (connection tube) between the load cell and shaker; 6—load cell (bonded to the panel); 7—acquisition data system; 8—computer and software for data processing.
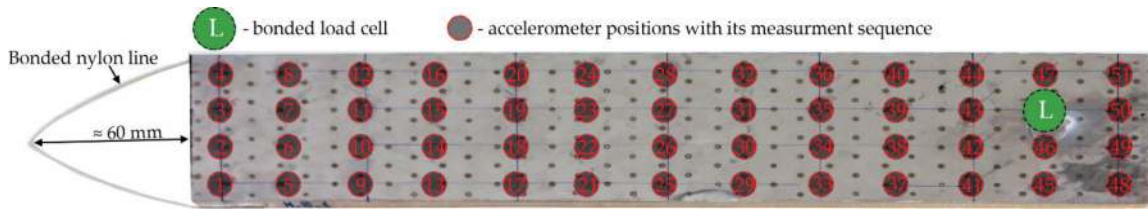
Figure 8. 51 mesh sequential point positioning of the accelerometer in a small-sized FMLP MPin-C-MPin hexagonal 10 mm type (≈350 × 80 × 4 mm).

Figure 9 shows the FRF curve typical of the amplitude and phase relationship (angular lag) along the frequency domain (0–800 Hz) between the output signals (measured acceleration) and input (applied force), from which the dynamic properties of the panels were determined. In this case, the phase between the responses of the accelerometer (acceleration) and the load cell (force) has a role to confirm if a resonant peak actually occurred along the frequency domain. Rao [12] mentions that resonance occurs when simultaneously a peak in the positive signal of FRF amplitude is observed and when the phase is near or passes through 90°. As shown in **Figure 9**, in the four resonance peaks (modes) the phase signals clearly changed their values (downwards), thus, by confirming that the resonance peaks actually occurred. The shape of the peaks (resonances) also indicates the level of damping, since the more "oval" peaks are associated with high damping effect. The Rational Fraction Polynomial (RFP) method [11, 16] was used to accurately determine the natural frequencies (fn) and damping factors (ξn) of each mode. The RFP method consists in adjusting a ratio of polynomials to FRF curves (amplitude and phase) obtained experimentally. For this purpose, a routine was devised in MATLAB® environment.

The dashed lines of **Figure 9** point to the appearance (typical for all panels analyzed) of the adjustment made by the RFP method in FRF (amplitude and phase) experimental curves using a 7th degree polynomial. With the adjustment performed in all positions, 51 modal parameters of each panel, namely the natural frequencies (fn) and damping factors (ξn), were determined. The solid lines of **Figure 9** show the FRF curves of the amplitude and phase evaluated in a given position of the panel (similar behavior for the other points of the mesh). It is possible to note the presence of four peaks (frequencies around 200, 480, 560 and 650 Hz) from the amplitude plot of **Figure 9**, indicating the resonant frequencies of the panel.

Parts (a) and (b) of the **Figure 10** present average results of four modes of the natural frequency (fn) and damping factor (ξn), respectively, measured at the 51 points of the measurement mesh. To facilitate the analysis, **Table 2** was organized to display the results of the four modes of vibration in terms of natural frequency and damping factor for all types of pinned small-sized panels in relation to the conventional one (without pins). Regarding the natural frequency, which represents the relationship between the stiffness and mass of a structure, it is possible to notice that the pinned panels did not have a significant variation of the natural frequencies of the vibration modes compared to the panels without pins. This implies that the pins have little effect on this dynamic property. Possibly, in spite of the mass increase provided by the deposition of the pins, the increase in stiffness takes place in a proportional way so that the natural frequency remains unchanged (in relation to the panel without pins). In contrast, the presence of the pins in the FMLPs significantly increased the damping factor of the FMLPs between two and five times (pinned panels with 10 mm spacing and hexagonal deposition pattern) depending on the vibration mode, compared to conventional panel (without pins). This was probably due to the fact

that the pins, individually or group, acts as a power dissipation mechanism. Thus, the oscillation amplitudes are attenuated more quickly with the presence of the pins. This quality could be exploited in practice, for example, aiming at structures less susceptible to acoustic problems and to high amplitudes of vibration at low frequencies. Other patterns of deposition and/or pin density could be explored in the sense of improving acoustic insulation and damping characteristics of vibrations in structures based on metal-composite laminates.
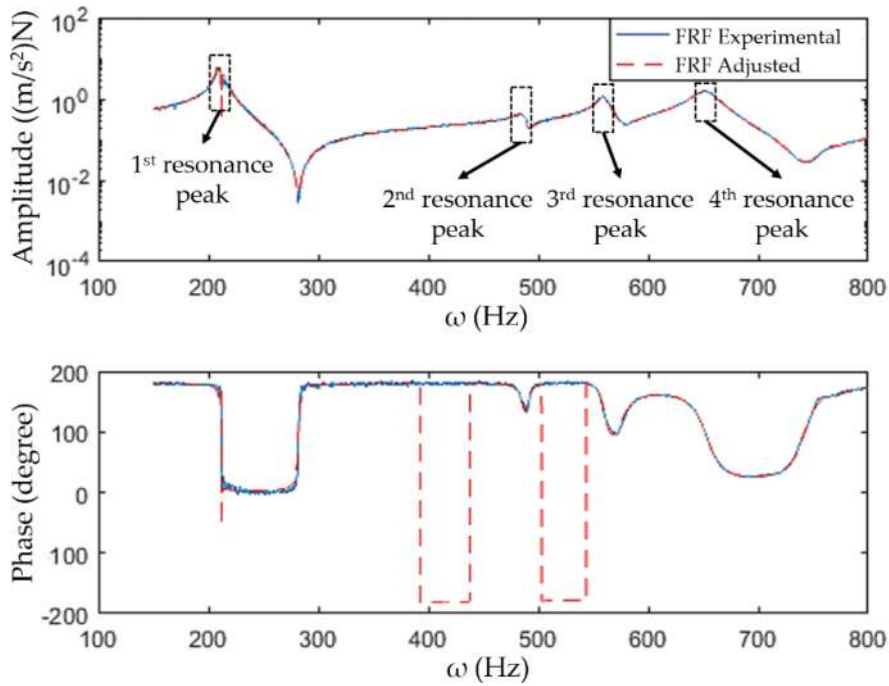
Figure 9. Amplitude (above) and phase (below) curves evaluated in a point of the MPin-C-MPin hexagonal 10 mm panel type (similar behavior for the other points), where solid lines are FRF and dashed lines are adjustment performed by the RFP method in the analysis band (ω) between 0 and 800 Hz (note that the adjustment overlapped the experimental curve for the amplitude case).
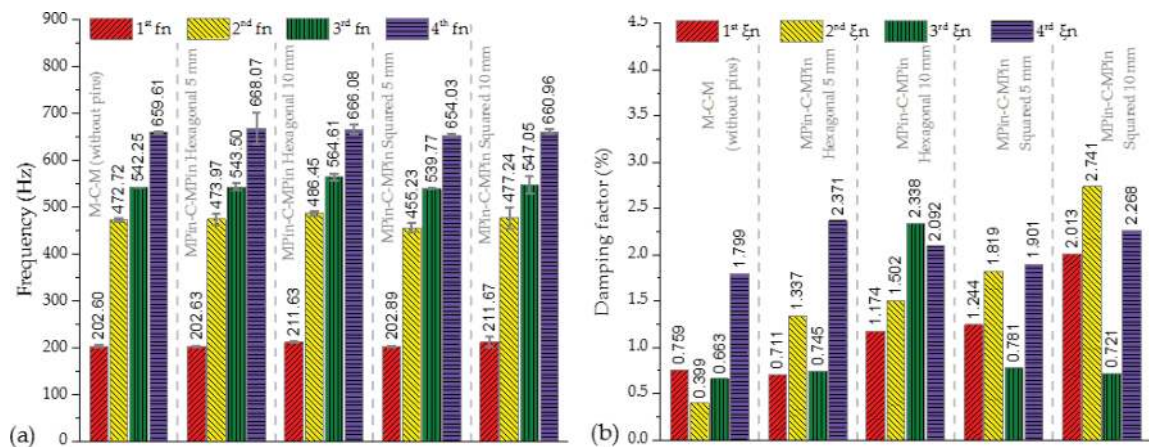

Figure 10. (a) Average results of the four natural frequency modes (fn) and (b) average results of the four modes of damping factors (ξn) obtained through modal analysis of the small-sized FMLPs.

Panel type	1st mode (%)		2nd mode (%)		3rd mode (%)		4th mode (%)	
	Δfn	Δξn	Δfn	Δξn	Δfn	Δξn	Δfn	Δξn
MPin-C-MPin hexagonal 5 mm	0.02	−6.32	4.46	54.68	0.14	63.90	4.48	165.22
MPin-C-MPin hexagonal 10 mm	0.26	235.09	2.90	276.44	−3.70	355.89	0.96	586.97
MPin-C-MPin squared 5 mm	0.23	12.37	4.12	252.64	−0.46	17.80	0.89	8.75
MPin-C-MPin squared 10 mm	1.28	31.80	0.98	16.29	−0.85	5.67	0.21	26.07

Table 2. Percentage change of vibration modes of the natural frequency (Δfn) and damping factor ($\Delta \xi n$) of the panels with pins in relation to the conventional panel (without pins).

3.2. Cosmetic characterization

In literature [17–19], the major part of Fiber-Metal Laminates (FMLs), due to their advantages, is used in modern aircraft parts, such as fuselage, wings, etc. FMLPs are used as manufactured or after paint application. In this context, the quality of the surface becomes a relevant factor. Thus, the objective of this section was to evaluate the influence of the deposition of the pins on the metal surface of the FMLP. A general evaluation of the cosmetic characteristics of the different FMLPs was made by measuring the waviness and roughness of the metal surfaces opposite to the pinned regions.

Figure 11 shows a small-sized FMLP reinforced with pins, where it is possible to perceive the dark marks on the metal surface, which represent the pins deposited on the opposite side. These marks are characterized by a localized deformation (peak and valley) and a heat-induced oxidation due to the welding of the pins (the cosmetic effect of the oxidation could be avoided with the application of purging with inert gas or reducing agent), that is, it is taken as a thermomechanical effect. The localized deformation is due to the operational mode of the CMT PIN, which deposits the pins by arc process (thermal effect), creating a small weld pool, but not reaching the opposite side. The tip of the electrode wire then penetrates into the weld pool, possibly reaching its bottom and pushing the surface of the metal sheet, deforming it (mechanical effect), characterizing the peak in the center of the marks (out of the panel). Then the current is turned off and the wire solidifies on the surface of the metal sheet. Next, current flows through the welded wire and metal sheet, promoting heating by Joule effect and wire softening, and a retraction movement of the wire breaks it apart, leaving behind a pin. It is believed that this retraction of the wire deforms the metal sheet, creating valleys concentric to the peak in the future panel. Concurrently, some expansion and contraction effects may also occur, but in a secondary way.

The measurements of surface waviness and roughness was performed with a Form Talysurf Intra profilometer from Taylor Hobson® with a resolution of 16 nm and range measurement of 1 mm. The measurement parameters were set as measuring speed equal to 0.25 mm/s, measuring length equal to 10 mm and ambient temperature of 20 ± 2°C (ABNT NBR ISO 1 [20]) and value of cut-off sample length equal to 0.8 mm (according to ISO 4288 [21]). Recalling that the cut-off value represents a segment of measurement length used in some representations of roughness measurements. It is important to note that, for the panels with pins, the tip of the profilometer was positioned to measure only some of the regions of marks left by the deposition of the pins crossing them

radially. In the panels without pins, areas of the same size were chosen. For statistical purposes, three samples of surfaces for each type of panel, chosen randomly, were analyzed. **Figure 12(a)** and **(b)** show the typical waviness profiles of the surfaces of panels with and without pins, respectively, and illustrates the associated measured region. The quantification of the waviness was made from the maximum distances between peak and valley [ΔZ of **Figure 12(a)**] of each marking. It has been observed that the peak of the surface corrugation profile is located in the center of the pin deposited on the opposite surface of the metal sheet and the two minimum peaks appear around the pin, as shown in **Figure 12(a)**. Since the pins are made with the same parameters, the values of ΔZ are close, resulting in an average value of 26.92 ± 2.35 μm. For comparison purposes, the same criterion was applied in FMLPs without pins, resulting in average ΔZ of only 1.40 ± 0.40 μm.

The column graph of **Figure 13** shows the average (Ra), maximum (Rz) and total (Rt) roughness of the sampled regions of the panels. Recalling that Ra is the arithmetic mean

Figure 11. Example of the dark marks on the metal surface of the small-sized FMLP (MPin-C-MPin hexagonal 5 mm with dimensions ≈350 × 80 × 4 mm) caused by pin deposition process.
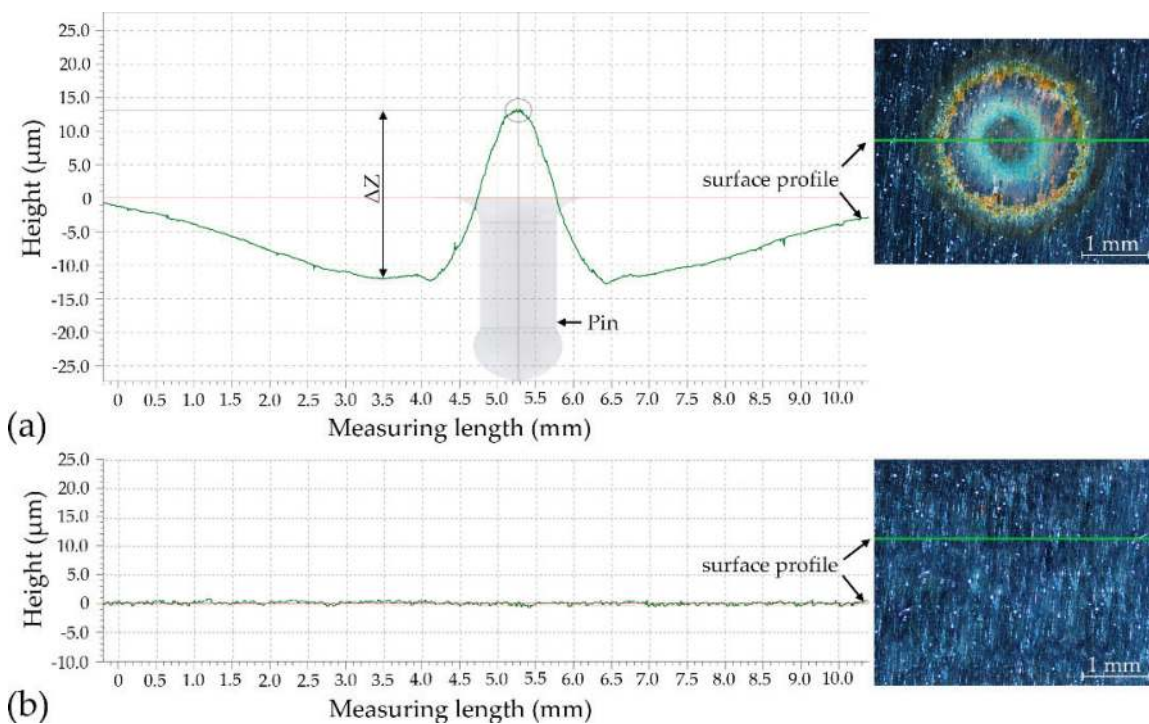

Figure 12. Typical surface profiles of the small-sized panels, where: (a) with pins (showing sharp waviness); (b) without pins (without waviness).
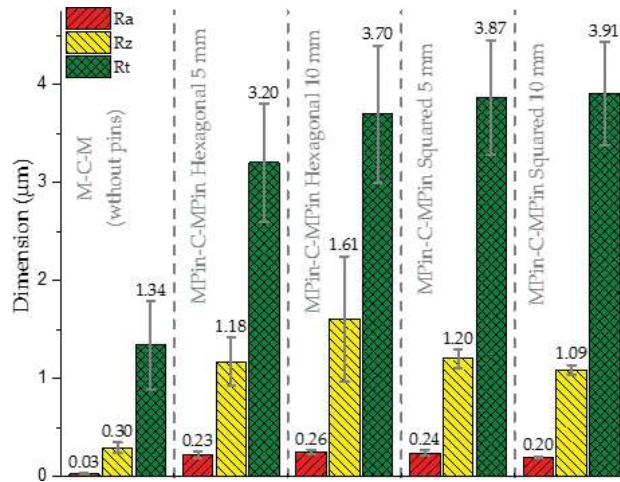
Figure 13. Results of Ra (mean), Rz (maximum) and Rt (total) obtained on small-sized FMLPs surfaces.

of the absolute values of the roughness peaks in relation to a midline within the measurement length. Rz is defined as the highest value of the roughness (peaks), that is, the roughness measured in segments defined by the cut-off, which is presented in the measuring path. Finally, Rt corresponds to the vertical distance between the highest peak and the deepest valley in the measurement length, obtained within the segments defined by the cut-off. These roughness representations were chosen based on the studies of De Chiffre et al. [22] and De Chiffre [23], which demonstrated the parameters most used in industry. The results show that all types of panels have roughly the same roughness values of Ra, Rz and Rt (considering the mean standard deviation). However, the deposition of the pins promoted an increase of roughness in the regions of the marks, in relation to the conventional panel.

Thus, it was concluded that the deposition of the pins by CMT PIN process, through its thermo-mechanical principle (electric arc with advancement and retraction of the wire), changes the surface profile of a metallic sheet (0.4 mm thickness), but only on a microscopic scale (at slightly less than 30 μm in terms of waviness and at just over 0.20 μm in terms of roughness). In this way, the elimination of staining due to pin deposition already largely removes the cosmetic drawbacks.

4. Destructive evaluation

In order to evaluate the influence of the pins as anchorages between metal and composite inside FMLPs, mechanical tests were employed until failure. Drop-weight test (low-speed impact test) was performed to assess the capacity of the FMLPs to dissipate impact energy. Buckling test, after impact (drop-weight test), was used to evaluate the performance of the FMLPs in such loading condition. And shear test (Iosipescu) was carried out to survey the effects that the pins have on the delamination of FMLPs.

4.1. Drop-weight testing

The FMLPs reinforced with pins, as conceived in this work, and the reference panels [M-C-M (without pins)] were submitted to impact damage by drop-weight testing. The small-sized FMLPs produced were cut in half their length, resulting in specimens of ≈175 × 80 × 4 mm each, and thus two specimens were used for each FMLP type. The aim with this test was to verify whether the pins would have positive or deleterious effects on the FMLPs concerning their capacity to absorb impact energy. Based on the ASTM D7136 standard [24], a rig to impose free fall (from around 1850 mm of height) of a constant mass (2.326 kg) over the small-sized panel surface was devised (**Figure 14(a)**). This mass was composed of a 28.5 mm spherical head made of hard steel attached to a plain carbon steel cylinder (50 mm of diameter and 150 mm of length). The rig included a latching device for ensuring no mass bouncing (single impact). A commercial high-speed camera filming at 2000 frames per second with 90 mm f/2.5 macro lens and frontal lighting was employed to quantify the energy (based on mass speed) involved in the impacts. The free fall height aimed a potential energy sufficient for causing apparent damage at impact, which resulted in 10.5 J per each millimeter of panel thickness (gravitational acceleration considered as 9.81 m/s^2). **Figure 14(b)** shows the upper and lower surfaces of all types of panels after impact.

High-speed images were used for determination of the falling/raising mass velocities immediately before/after impact, based on displacements (visualized from frame to frame) of its spherical head lower surface and respective time lapses, as seen in **Figure 15(a)**. A fitting curve, taking into account the non-uniform rectilinear motion due to gravity of the falling/raising mass, was figured out for each panel (including replications) and the velocities at the panel upper surface level were estimated by extrapolation. The velocity right at the end of the fall (actual impact) is referred as impact velocity and the velocity right at the beginning of the rebound as return velocity, which resultant average levels varied respectively from 5.81 to 5.96 m/s, as indicated in **Figure 15(b)**. According to Ursenbach et al. [25], the drop-weight test applied was classified as of low impact velocity (between 1 and 10 m/s). Farooq and Myler [26] consider an impact as of low velocity when an object impacts a target without penetrating it, situation observed for all panels tested in this present work.

The velocities involved in the impacts, in turn, were used to calculate the impact and return energies. Impact energy was considered as the kinetic energy of the falling mass just before actual impact (fall height tending to zero–panel upper surface level before impact). Analogously, return energy was taken as the kinetic energy of the raising mass at the beginning of the rebound after the impact (rebound height tending to zero–panel upper surface level before impact). Energy dissipation during impact was assumed as the relative drop in the kinetic energy due to impact. The impact energy quantities were represented by two ways: energy and specific energy (considering the panel mass density), as presented in **Figure 16**. As seen, the impact energy was always around 40 J, being the small fluctuation probably due experimental errors. The return energies and energy dissipations were also similar for all FMLPs types. In general, the presence of pins as anchorages inside the FMLPs did not seem to have any significant effect concerning the capacity of the panels to absorb impact energy. Therefore, the pins, at least for the impact conditions applied, did not make the FMLPs more brittle. In addition, the change in the deposition pattern of the pins, at least for the remaining conditions, did not show any effect concerning the capacity of the panels to dissipate impact energy.
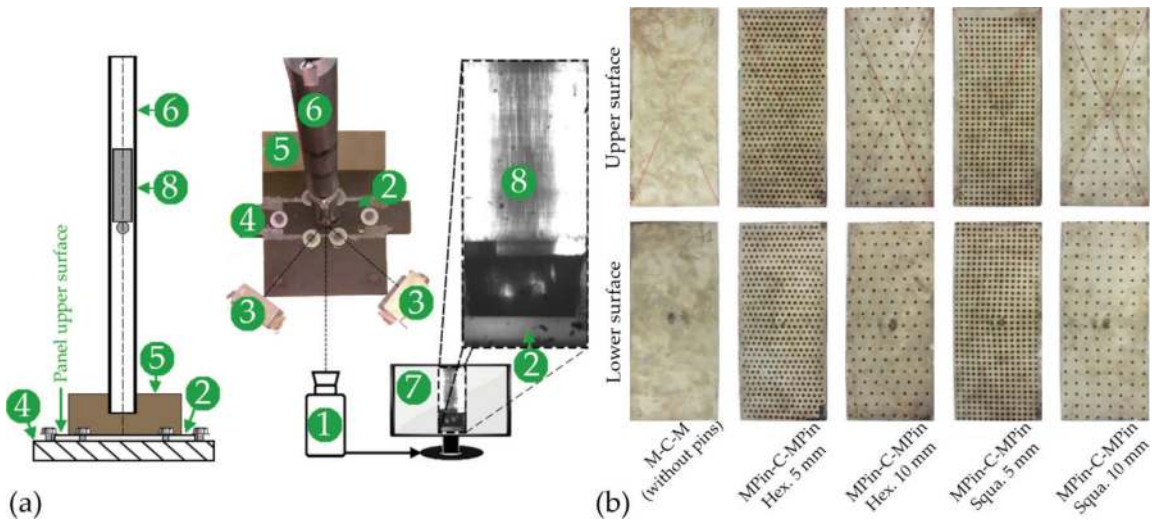
Figure 14. (a) Schematic frontal and top views of the drop-weight test rig, where: 1—high-speed camera with lens; 2—small-sized panel; 3—halogen lamp of 1 kW (2 units); 4—high-inertia base with central clearance hole (125 mm long, 75 mm wide and 25 mm deep); 5—flat background, perpendicular to the base; 6—mass guidance tube; 7—PC for image viewing; 8—mass with spherical head; (b) upper and lower surfaces of all types of panels (≈175 × 80 × 4 mm) after impact.
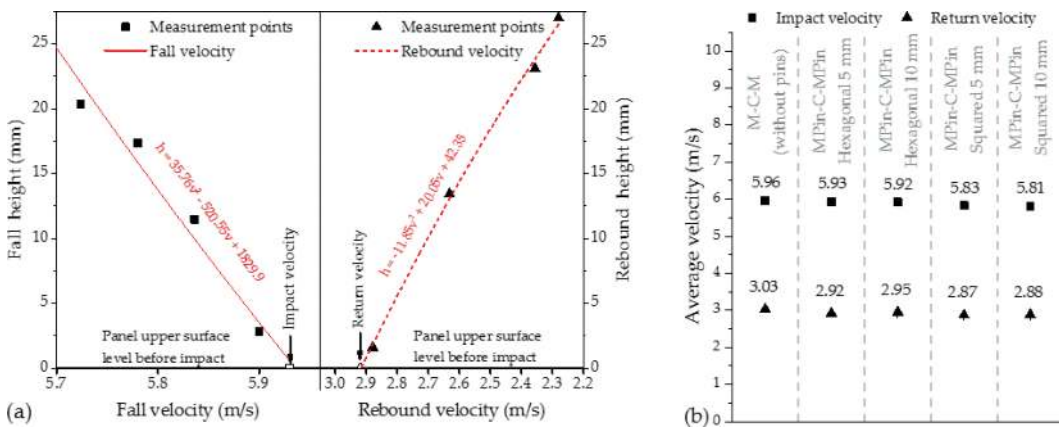

Figure 15. (a) Extrapolation of the falling/raising mass velocity at impact and return (MPin-C-MPin hexagonal 5 mm panel, as example); (b) average impact and return velocities for each panel (h = height; v = velocity).

4.1.1. Damage characterization (damage depth profile) after impact

The through-thickness damage extent, i.e., the depth profile of the impact damage (permanent deformation), was found by measuring the vertical displacement of the central transversal and central longitudinal lines drawn in all panels before drop-weight testing. The edges of the panels, both in length and width, were taken as references without permanent deformation after impact. A commercial manual-floating-type coordinate measuring machine, with 1 μm of resolution, was used for taking the measurements. The damage profile was determined by scanning the upper and lower surfaces of the panels, as exemplified in **Figure 17**. As seen, the measuring mesh was reduced to 5 mm near the damage area, against 10 mm in the rest of the surface of the panels.
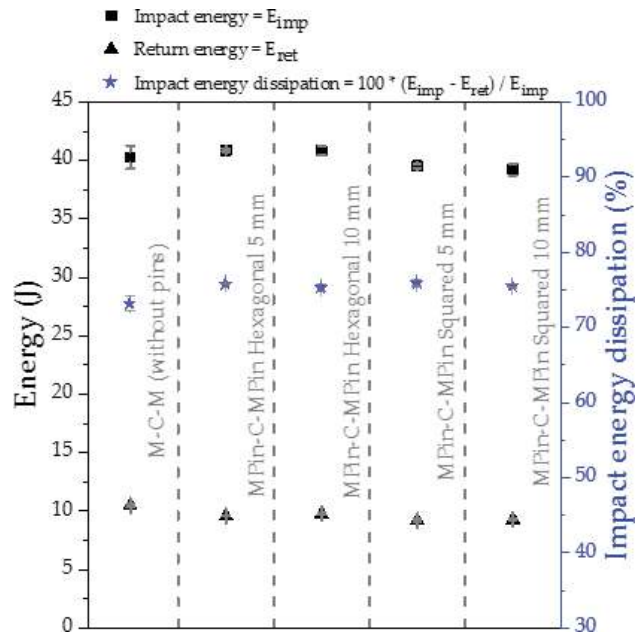
Figure 16. Average impact and return energies and consequent energy dissipation during drop-weight testing.
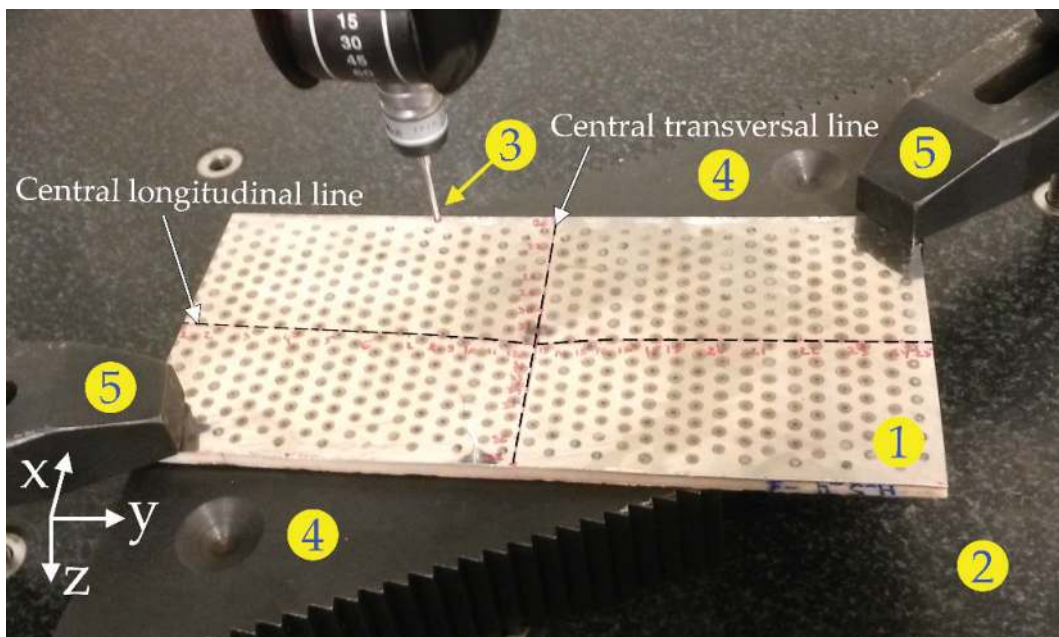

Figure 17. General setup for damage depth profile determination (upper panel surface, as example), where: 1—damaged small-sized panel (MPin-C-MPin hexagonal 5 mm panel, as example); 2—work table; 3—3D digital probe (touching head); 4—support; 5—clamping.

The average damage depth profiles of each panel are shown in **Figure 18(a)**. As the profiles were nearly longitudinally and transversally symmetrical, only half of the panel's length and width are represented. In general, the damage profiles found in each surface of the FMLPs with pins were similar, longitudinally as well as transversally, to the profiles found in the conventional

FMLP [M-C-M (without pins)]. However, the presence of pins tends to change the permanent deformation of the panels after impact as complementarily shown in **Figure 18(b)**. It is also noted that the upper and lower surfaces exhibited different typical deformation profiles. In all panel types, the depth profile was more concentrated (shorter and shallower) in the upper surface than in the lower surface. The falling mass head might have tended to replicate its spherical contour on the upper surface, with the extent limited by the panel own thickness, which would work as restriction against deformation. The final damage extent at the lower surface, in contrast, is limited by the edges of the central clearance hole of the base of the drop-weight test rig, which are reasonably far away. It is even possible to observe that the change in damage depth profile is more gradual along the central longitudinal line (edges of support 125 mm apart) and more abrupt along the central transversal line (edges of support 75 mm apart). As the conventional FMLPs [M-C-M (without pins)] and FMLPs with pins had equal number of prepreg layers, they behaved similarly, consequently dissipating a close amount of energy during impact (**Figure 16**).

For a better understanding of the results of the least permanent deformed FMLPs, MPin-C-MPin squared 5 mm and MPin-C-MPin hexagonal 10 mm (**Figure 18(b)**), they were analyzed visually. In **Figure 19**, it is possible to notice that, in the case of these FMLPs, the spherical
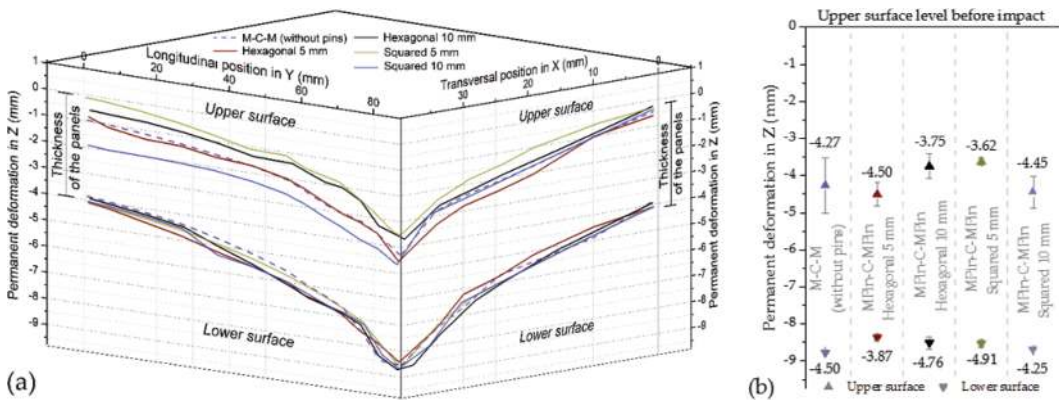

Figure 18. (a) Depth profiles of the damages produced in each panel (average of 2 samples) from 3D digital probing; (b) average maximum permanent deformation in each panel.
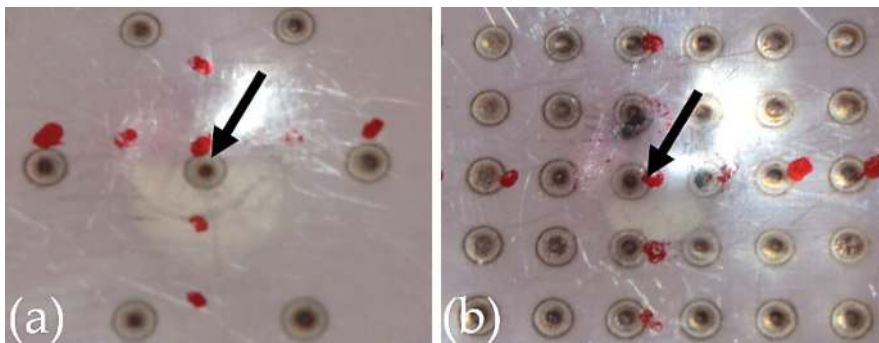

Figure 19. Zoom of the impact region of the upper surfaces of specific FMLPs after the drop-weight test, where: (a) MPin-C-MPin hexagonal 10 mm; (b) MPin-C-MPin squared 5 mm (the arrow indicates the deepest location of the panel after impact deformation).

head of the impactor reached the surface region with the deposited pin. In turn, this caused less permanent deformation in the panels with pins in comparison to the others. This indicates the pins acted holding the metal sheet to the composite, restraining delamination and external deformation.

4.2. Buckling after impact

According to Ishikawa et al. [27] and De Freitas and Reis [28], the resistance of composite panels to in-plane compressive stresses is strongly impaired by the presence of delamination-type damages, culminating in expressive reductions in buckling resistance of components. In that way, all types of FMLPs were subjected to buckling test after impact (drop-weight test) as investigation on the influence of pins on damage tolerance. For each type of small-sized FMLP two samples were tested for buckling. An electromechanical universal testing machine was used. Upper and lower supports for the panels were designed and built to allow proper alignment and fixture for the test, as shown in **Figure 20**. In accordance with ASTM D7137 standard [29], the testing speed (upper head moving rate) was always set at 1.25 mm/min.

Figure 21(a) shows the general evolution of axial displacement *versus* load in the buckling tests of all types of FMLPs after impact damage with compression, buckling and failure phases as detailed by Skhabovskyi et al. [10]. The mean values resulting from two tests of maximum compressive load, failure load, axial displacements at maximum load and failure are shown in **Figure 21(b)**. The axial displacement of the failure is shown as an alternative correlated with the lateral deflection of the panels tested. As seen, pinned FMLPs tolerated a higher maximum load, having close performances with each other, except the MPin-C-MPin squared 10 mm panel, which was able to withstand a smaller maximum load but still larger compared to the conventional panels [M-C-M (without pins)].
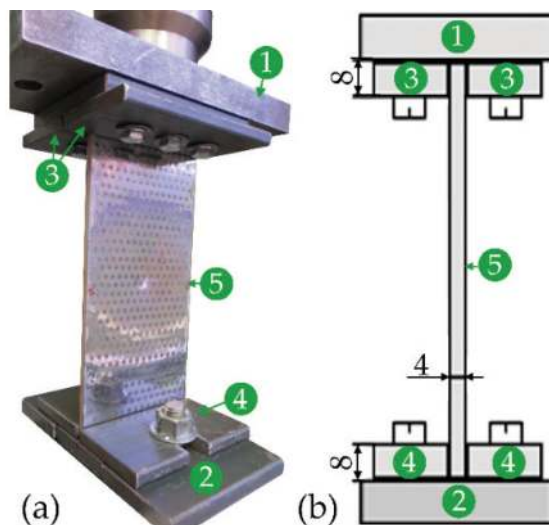

Figure 20. (a) Image of small-sized FMLP (MPin-C-MPin hexagonal 5 mm, as example) assembled in the testing machine; (b) schematic side view of the buckling set up, where: 1—moving upper head; 2—fixed lower head; 3—upper support (two parts); 4—lower support (two parts); 5—panel; 6—support fixture side plates; 7—auxiliary holding bar; 8—auxiliary clamps (dimensions in mm).
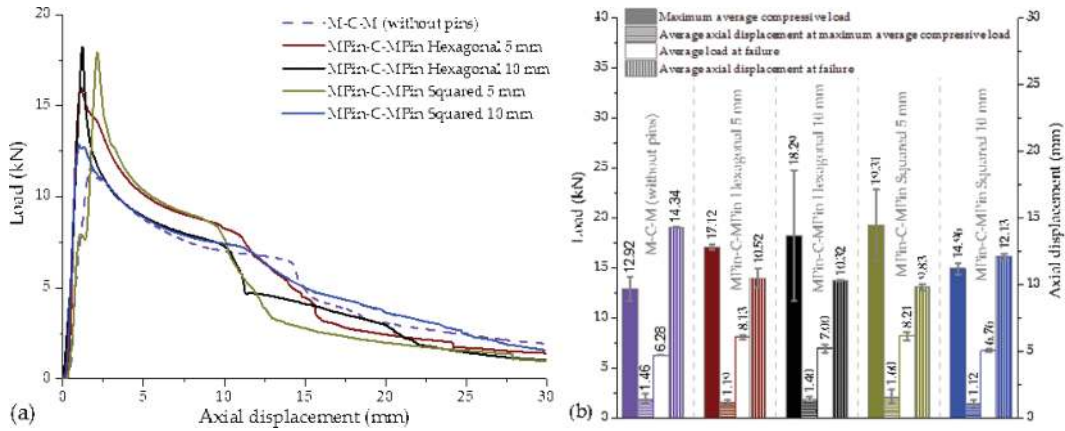
Figure 21. (a) Typical evolution of axial displacement *versus* load in buckling tests of all types of panels after impact damaging; (b) maximum average compressive load, average load at failure and correspondent axial displacements after buckling tests of all types of panels after impact damaging.

All types of the FMLPs achieved loads of maximum compression around 1.35 mm of axial displacement. **Figure 21(a)** shows that FMLPs with higher pin density (5 mm spacing) were able to withstand higher loads during deflection (buckling phase), followed by pinned panels in lower spacing patterns (panels MPin-C-MPin squared 10 mm and MPin-C-MPin hexagonal 10 mm in this order). As shown in **Figure 21(a)**, conventional FMLPs (without pins) reached a high load value at failure, still with a high axial displacement value at this moment, compared to FMLPs with pins. However, conventional FMLPs (without pins), after reaching a high value of failed load, showed a rapid unloading after the rupture (catastrophic failure).

MPin-C-MPin squared 5 mm and MPin-C-MPin hexagonal 10 mm panels supported higher maximum compression and failure loads (**Figure 21(b)**), probably because of their lower maximum permanent deformation (**Figure 18(b)**). It was also noted that MPin-C-MPin squared 5 mm and MPin-C-MPin hexagonal 10 mm panels did not show a good repeatability of their high mean maximum compressive load, as evidenced by a high average standard deviation in **Figure 21(b)**. This probably happened because the spherical head of the impactor hit the pin region in one of two tests performed, thus leading to the smallest deformation. The other FMLPs showed similar permanent deformation, which is supported by good repeatability of the loads and displacements in the buckling test. In this case, the pins possibly tend to retard the propagation of debonding between metal sheets and composite, for anchoring them to each other, and even tend to retard the spread of delamination in the composite, for acting as clamps that hold most of its layers together between the metal sheets and pins ball-heads. That is, the pins tend to delay the propagation of the delamination between the metal sheets and the composite by their anchoring and even tend to delay the propagation of the delamination in the composite, acting as staples that support most of their layers between the metal sheets and ball-head pins.

Figure 22 shows the images of all types of panels with impact damage after the buckling test. As expected, all types of panels had their lateral deflection going from the upper surface (side of impact) towards the lower surface. All panels collapsed and ended folded with presence of corrugations transversally crossing the areas of damage. Still all FMLPs had the lower metal sheet
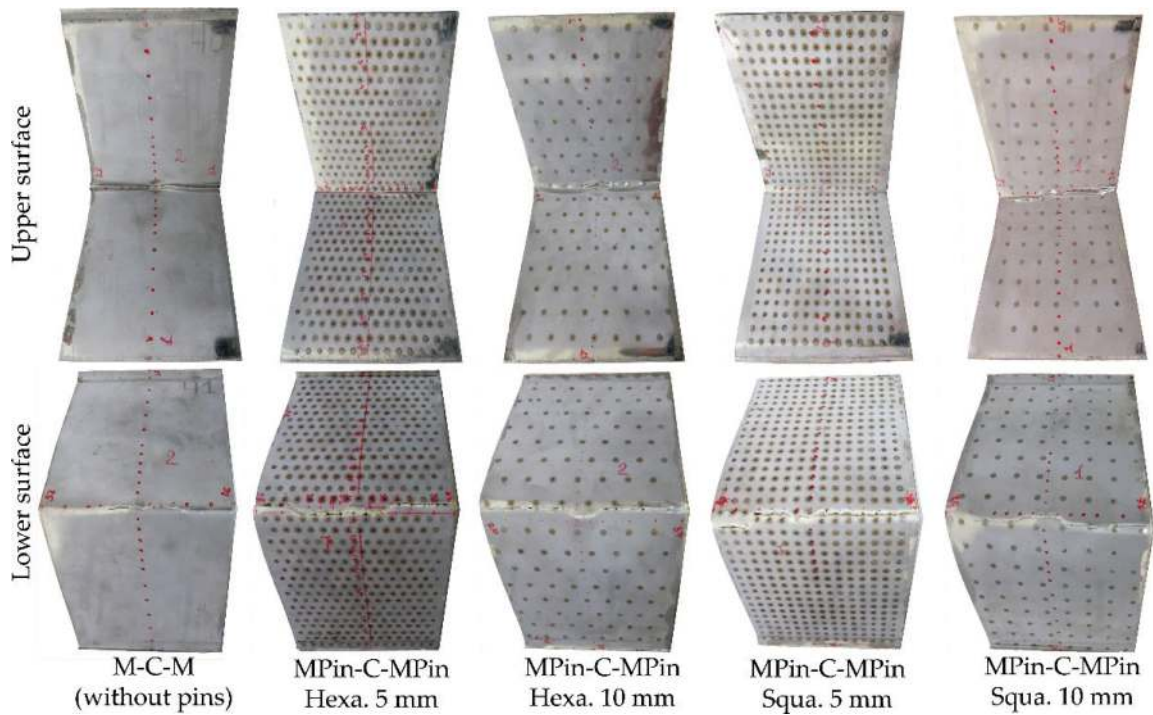
Figure 22. Typical appearance of all types of FMLPs with impact damage after buckling test.

ruptured transversely in the middle after the buckling test, including the conventional panel (without pins). But in the case of M-C-M (without pins), the fracture did not cross the entire width of the panel, concentrating closer to the damage region (**Figure 22**). It was also noticed that the ruptures of the metallic sheets happened between the metallic pins (spacings), because the pins acted as anchoring of the metallic sheets and because the tensile tensions were present in the inferior metallic sheets (side opposite to the impact) between the pins. It was noted that the M-C-M type panels (without pins) with impact damage ended the buckling test with the metal sheets slightly separated from the composite. In contrast, the FMLPs with pins exhibited metal sheets-composite debonding notably concentrated around the damage areas. This fact ratifies that the pins effectively anchor the metal sheets to the composite, even after impact damage.

4.3. Iosipescu shear test

To evaluate the influence of the deposition of the pins in the FMLP on shear and delamination resistance, a shear strength test was used, as proposed for the first time in 1967 by Iosipescu. According to Le Bourlegat [30], the Iosipescu shear test uses a simple test body because it is flat and achieves a pure and uniform shear stress-strain state in the region of the notch imposed on the specimen. **Figure 23(a)** shows a simplified view of this test performed on the universal machine for mechanical testing. **Figure 23(b)** shows the dimensions of the specimen used and defined by ASTM D5379 standard [31]. In addition, every Iosipescu shear test procedure was based on this standard, keeping the movable jaw displacement speed equal to 0.5 mm/min. The test was carried out on five specimens taken from each of the five
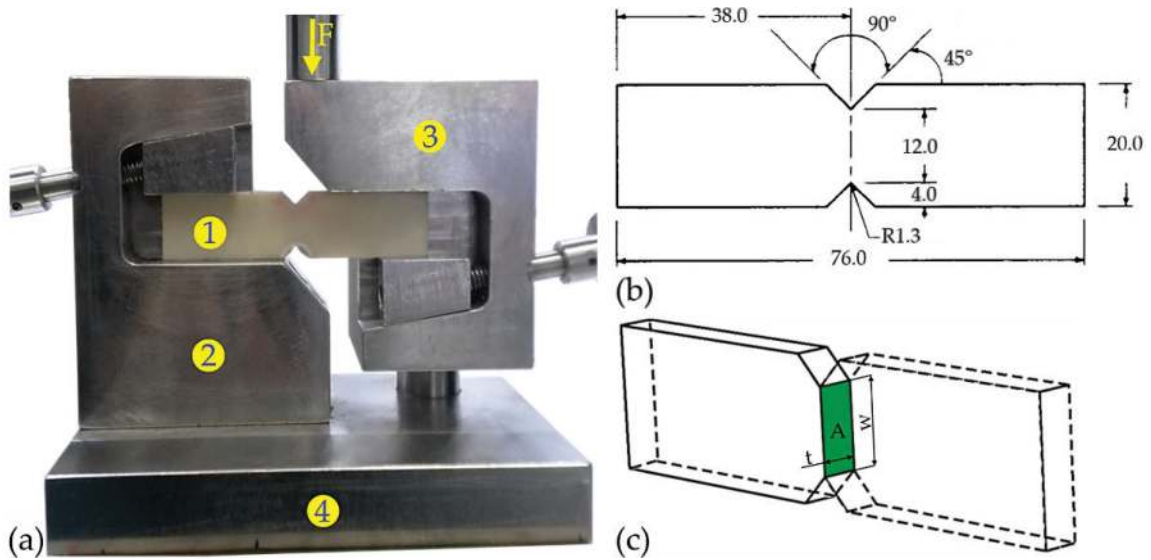
Figure 23. (a) Simplified view of the Iosipescu shear test, where: 1—specimen; 2—fixed jaw; 3—mobile jaw; 4—base; F—applied load; (b) dimensions (in mm) of the specimens used in the Iosipescu shear test (adapted from ASTM D5379 standard [31]); (c) area of the specimen used for shear stress calculations (adapted from Le Bourlegat [30]).

types of small-sized FMLPs. **Figure 23(c)** shows the area (A) of the plane between the notches of the specimen (w ≈ 12 mm and t ≈ 4 mm) along which the load (F) was applied. To calculate the shear stress (τ), Eq. (1) was used.

$$\tau = \frac{F}{w * t} \tag{1}$$

Figure 24 presents the typical appearance of FMLPs specimens before and after the Iosipescu shear test. **Figure 25** shows typical displacement *versus* load curves, respectively, for each type of panel in the Iosipescu shear test. During the tests a good repeatability of the results was observed for each of the five types of FMLPs specimens. **Figure 26** shows column diagrams with average values of maximum load, maximum load displacement, and maximum shear stress. It is observed that the specimens of the panels with the largest number of pins (5 mm spacing), regardless of their deposition pattern, showed the highest average maximum load (≈6.61 kN). The panels with lower pin density (10 mm spacing) exhibited a maximum load a bit lower (≈5.83 kN), regardless of the deposition pattern. Finally, the conventional FMLP specimens [M-C-M (without pins)] showed the lowest maximum load (≈5.04 kN), approximately 25% below the results with the specimens of the panels with spacing of 5 mm.

The specimens of FMLPs with pins reached a maximum load displacement of approximately 2.91 mm (**Figure 26**), except for the specimens of the MPin-C-MPin squared 10 mm panel that showed a lower displacement value at the moment of failure (1.44 ± 0.06 mm). This probably happened because of the pin position inside both notches (**Figure 24**). As there was a pin very close to the edge of the notch, there may have been stress concentration right at this point, thus breaking the specimens of this case in advance and leaving no room for further displacements.
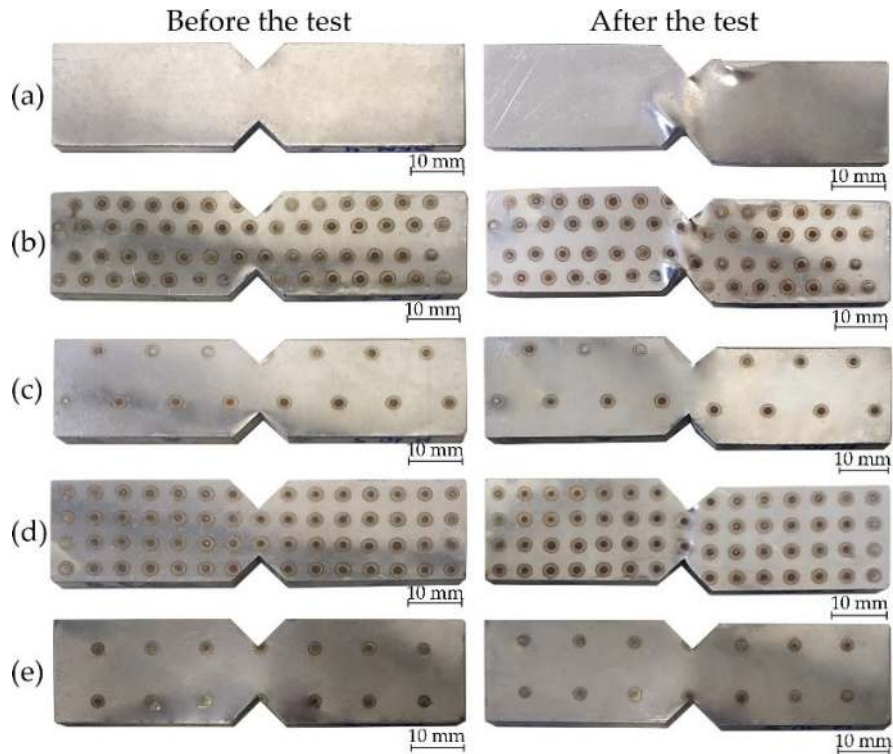
Figure 24. Typical aspect of the five types of FMLPs specimens before (left) and after (right) the Iosipescu shear test, where: (a) M-C-M (without pins); (b) MPin-C-MPin hexagonal 5; (c) MPin-C-MPin hexagonal 10; (d) MPin-C-MPin squared 5; (e) MPin-C-MPin squared 10.
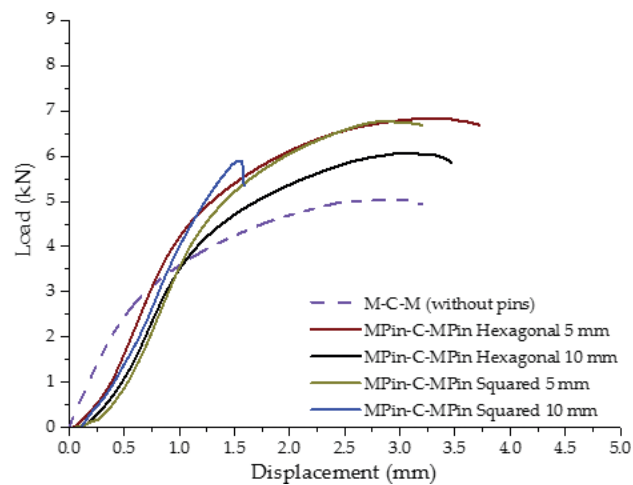

Figure 25. Typical displacement *versus* load curves for each FMLP type in the Iosipescu shear test.

In general, the panels with pins showed better results of maximum load, demanding a higher value of shear stress to break. Probably, this result was caused because the contact between the metallic sheets and the composite of the pinned specimens are more anchored due to the presence of the pins. In such a way, the greater number of pins (5 mm spacing) provided
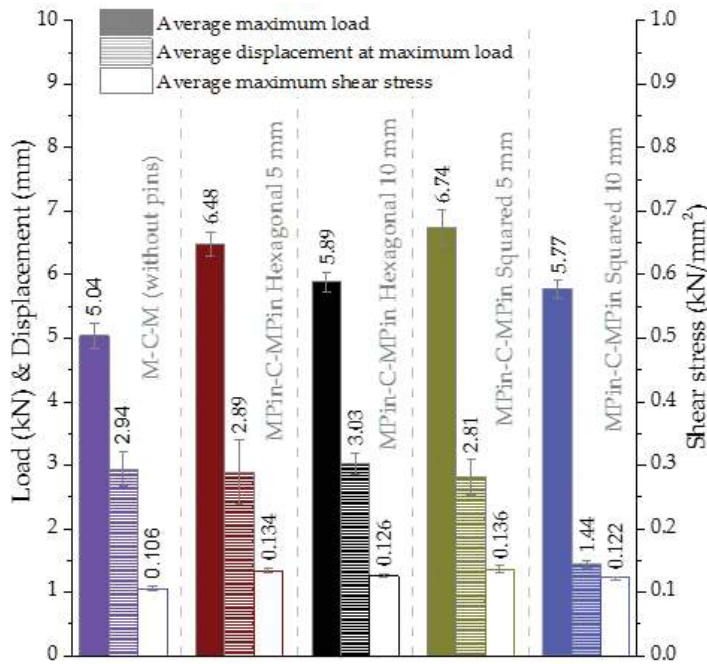
Figure 26. Average results obtained through five measurements of maximum load, displacement at maximum load and maximum shear stress of the Iosipescu shear test.

a better union, consequently showing better results. Possibly, failures in pinned specimens would be less catastrophic after reaching the maximum load (after failure), which should be exploited in future work.

5. Conclusions

Considering the conditions applied in the evaluation of pins deposited by CMT PIN process in FMLPs, the following conclusions are listed according to the type of testing.

Non-destructive evaluation:

- By means of the four natural frequency modes obtained after the modal analysis, the presence of the pins in the FMLPs did not result in a significant stiffness increase. There are, in this case, probably two factors acting in opposite directions; the pins would lead to an increase in stiffness due to the anchoring action between metal and composite, but on the other hand the mass increase with more pins inside the panels is a stiffness-reducing factor as in any structure. However, the presence of the pins in the FMLPs significantly increased the damping factor, dissipating the applied vibration wave. Pin deposition was able to reduce the propagation of vibrations at low frequencies (from 0 to 800 Hz) by up to about five times (for some resonance modes).

- CMT PIN process, through its thermo-mechanical working principle, changes the surface profile of the metal sheets on the opposite face in the region of deposition, but only on a microscopic scale. In addition, thermoxidation occurs in these regions, which is not a problem because this inconvenience could be avoided/minimized by the application of purge gas (supplementary protection to that used near the electric arc and inert).

Destructive evaluation:

- In terms of impact energy dissipation, all FMLPs with pins exhibited similar performance, generally equivalent to the conventional FMLP (without pins). Besides, the addition of weight by the pins as anchorages does not penalize the capacity of the panels to dissipate impact energy, as all panel types dissipated similar levels of specific energy during impact. Therefore, the pins did not make the FMLPs more brittle and the change in their deposition pattern did not show any significant effect concerning the capacity of the panels to dissipate impact energy.

- Concerning the damage depth profiles caused by drop-weight testing, all FMLPs with pins suffered damages similar to that found in the conventional FMLP (without pins).

- Regarding damage tolerance, the FMLPs with pins exhibited a less catastrophic trend, i.e., achieving significantly higher loads at longer axial displacements in buckling test after impact and the pins tend to retard the debonding propagation between metal sheets and composite, for anchoring them to each other. The pins also hold back the delamination spreading in the composite, for clamping the layers together between the metal sheets and ball-heads of the pins.

- The anchoring effect the pins have on the FMLPs was confirmed through the Iosipescu shear test. Generally, the panels with pins exhibited higher shearing loads in relation to the conventional panel (without pins). The FMLPs with the highest number of pins (5 mm spacing), regardless of the deposition pattern, presented the highest maximum loads and displacements at the moment of failure.

Acknowledgements

Author details

Ruham Pablo Reis[1]*, Iaroslav Skhabovskyi[1], Alberto Lima Santos[2], Leonardo Sanches[1], Edson Cocchieri Botelho[2] and Américo Scotti[1,3]

*Address all correspondence to: ruhamreis@mecanica.ufu.br

1 Centro Para Pesquisa e Desenvolvimento de Processos de Soldagem—LAPROSOLDA, Universidade Federal de Uberlândia—UFU, Uberlândia, Brazil

2 Departamento de Tecnologias e Materiais, Universidade Estadual Paulista—UNESP, Guaratinguetá, Brazil

3 Department of Engineering Science, Production Technology West, Division of Welding Technology, University West, Trollhättan, Sweden

References

[1]   Cortes P, Cantwell WJ. The prediction of tensile failure in titanium-based thermoplastic fibre-metal laminates. Composites Science and Technology. 2006;**66**:2306-2316. DOI: 10.1016/j.compscitech.2005.11.031

[2]   Sinmazçelik T, Avcu E, Bora MÖ, Çoban O. A review: Fibre metal laminates, background, bonding types and applied test methods. Materials and Design. 2006;**32**:3671-3685. DOI: 10.1016/j.matdes.2011.03.011

[3]   Salve A, Kulkarni R, Mache A. A review: Fiber metal laminates (FML's)—Manufacturing, test methods and numerical modeling. International Journal of Engineering Technology and Sciences (IJETS). 2016;**6**:71-84. DOI: 10.15282/ijets.6.2016.10.2.1060

[4]   Seydel R, Chang F. Impact identification of stiffed composite panels: I. System development. Smart Materials and Structures. 2001;**10**:354-369. PII: S0964-1726(01)18317-5

[5]   Vlot A. Impact loading on fibre metal laminates. International Journal of Impact Engineering. 1996;**18**:291-307. DOI: 10.1016/0734-743X(96)89050-6

[6]   Jahn J, Weeber M, Boehner J, Steinhilper R. Assessment strategies for composite-metal joining technologies—A review. Procedia CIRP. 2016;**50**:689-694. DOI: 10.1016/j.procir.2016.05.034

[7]   Fronius. Current Welding Practice: CMT Technology. 1st ed. Düsseldorf: DVS Media GmbH; 2014. 96 p. ISBN: 978-3-945023-36-5

[8]   Ucsnik S, Scheerer M, Zaremba S, Pahr HD. Experimental investigation of a novel hybrid metal-composite joining technology. Composites Part A: Applied Science and Manufacturing. 2010;**41**:369-374. DOI: 10.1016/j.compositesa.2009.11.003

[9]   Graham DP, Rezai A, Baker D, Smith PA, Watts JF. The development and scalability of a high strength, damage tolerant, hybrid joining scheme for composite-metal structures. Composites Part A: Applied Science and Manufacturing. 2014;**64**:11-24. DOI: 10.1016/j.compositesa.2014.04.018

[10] Skhabovskyi I, Batista NL, Damato CA, Reis RP, Botelho EC, Scotti A. Appraisal of fiber-metal laminate panels reinforced with metal pins deposited by CMT welding. Composite Structures. 2017;**180**:263-275. DOI: 10.1016/j.compstruct.2017.07.043

[11] Leme LMM. Estudo comparativo de técnicas de análise modal experimental no domínio da frequência em uma barra na condição de contorno livre-livre [trabalho de conclusão de curso]. Pato Branco: Universidade Tecnológico Federal do Paraná; 2014. Available from: http://repositorio.roca.utfpr.edu.br/jspui/bitstream/1/6094/1/PB_DAMEC_2014_2_03.pdf Accessed: Apr 23, 2017

[12] Rao SS. Vibrações Mecânicas. 4th ed. São Paulo: Pearson Prentice Hall; 2008. 424 p. ISBN: 978-85-7605-200-5

[13] Bolina CC, Palechor EUL, Vásquez MPR, Nicacio WG, Gutierres, MPD, Lopez AAO. Vibrações: as frequências naturais estimada e experimental de uma estrutura. In: Congresso Nacional de Matemática Aplicada à Indústria (CNMAI); Caldas Novas, Brasil; Nov 18-21, 2014. p.1-5. Blucher Ed. Available from: http://pdf.blucher.com.br.s3-sa-east-1.amazonaws.com/mathematicalproceedings/cnmai2014/0038.pdf [Accessed: Apr 23, 2018]

[14] Lundkvist A. Modal Analysis Project [Internet]. 2010. Available from: http://www.student.ltu.se/~nadlun-5/pdfs/l7005a_report_main.pdf [Accessed: Apr 23, 2018]

[15] Soeiro NS. Análise Modal Experimental [Internet]. 2001. Available from: http://www.ebah.com.br/content/ABAAAgT_QAK/analise-modal-experimental [Accessed: Apr 23, 2018]

[16] Richardson MH, Formenti DL. Parameter estimation from frequency response measurements using rational fraction polynomials. In: 1st Proceedings of the International Modal Analysis (IMAC) Conference; November 1982; Orlando. USA. 1982. pp. 1-15. Available from: http://citeseerx.ist.psu.edu/viewdoc/download?doi=10.1.1.458.3592&rep=rep1&type=pdf [Accessed: Apr 23, 2018]

[17] Laliberte JF, Poon C, Straznicky PV, Fahr A. Applications of fiber-metal laminates. Polymer Composites. 2000;**21**:558-567. DOI: 10.1002/pc.10211

[18] Marsh G. Composites lift off in primary aerostructures. Reinforced Plastics. 2004;**48**: 22-27. DOI: 10.1016/S0034-3617(04)00193-6

[19] Botelho EC, Silva RA, Pardini LC, Rezende MC. A review on the development and properties of continuous fiber/epoxy/aluminum hybrid composites for aircraft structures. Materials Research. 2006;**9**(3):247-256. DOI: 10.1590/S1516-14392006000300002

[20] Associação Brasileira de Normas Técnicas. ABNT NBR NM ISO 1. ABNT Ed. Temperatura padrão de referência para medições industriais de comprimento. Brasília, DF: 1997

[21] Associação Brasileira de Normas Técnicas. ABNT NBR ISO 4288. ABNT Ed. Especificações geométricas do produto (GPS)—Rugosidade: Método do perfil—Regras e procedimentos para avaliação de rugosidade. Brasília, DF: 2008

[22] De Chiffre L, Lonardo P, Trumpold H, Lucca DA, Goch G, Brown CA, Raja J, Hansen HN. Quantitative characterization of surface texture. CIRP Annals—Manufacturing Technology. 2000;**49**(2):635-352. DOI: 10.1016/S0007-8506(07)63458-1

[23] De Chiffre L. Industrial survey on ISO surface texture parameters. CIRP Annals—Manufacturing Technology. 1999;**48**(3):74-77

[24] American Society for Testing and Materials. ASTM D7136/D7136M-15. Standard Test Method for Measuring the Damage Resistance of a Fiber-Reinforced Polymer Matrix Composite to a Drop-Weight Impact Event, West Conshohocken, PA. In: Annual Book of ASTM Standards. 2015

[25] Ursenbach DO. Penetration of CFP laminates by cylindrical indenters [thesis]. The University of British Columbia. Vancouver, Canada; 1995. Available from: https://open.library.ubc.ca/cIRcle/collections/ubctheses/831/items/1.0078475 [Accessed: Aug. 03, 2018]

[26] Farooq U, Myler P. Finite element simulation of damage and failure predictions of relatively thick carbon fibre-reinforced laminated composite panels subjected to flat and round noses low velocity drop-weight impact. Thin Walled Structures. 2016;**104**:82-105. DOI: 10.1016/j.tws.2016.03.011

[27] Ishikawa T, Sugimoto S, Matsushima M, Hayashi Y. Some experimental findings in compression-after-impact (CAI) tests of CF/PEEK (APC-2) and conventional CF/EPOXY flat plates. Composites Science and Technology. 1995;**55**:349-363. DOI: 10.1016/0266-3538(95)00079-8

[28] De Freitas M, Reis L. Damage growth analysis of low velocity impacted composite panels. Composite Structures. 1997;**38**(1-4):509-515. DOI: 10.1016/S0263-8223(97)00086-X

[29] American Society for Testing and Materials. ASTM D7137/D7137M-12. Standard Test Method for Compressive Residual Strength Properties of Damaged Polymer Matrix Composite Plates, West Conshohocken, PA. In: Annual Book of ASTM Standards. 2012

[30] Le Bourlegat LR. Processamento e Caracterização Híbrido Titânio/Fibra de Carbono/Epóxi [thesis]. São José dos Campos: Instituto Tecnológico de Aeronáutica (ITA); 2009

[31] American Society for Testing and Materials. ASTM D5379/D5379M-12. Standard Test Method for Shear Properties of Composite Materials by the V-Notched Beam Method, West Conshohocken, PA. In: Annual Book of ASTM Standards. 2012